Research Advances

The Greenhouse Climate Records from Organic Carbon Isotope Excursions During the Toarcian (Early Jurassic) Sediments in the Shuanghu Area, Qianghai-Tibetan Plateau

YI Haisheng[1, *], JI Changjun[2, 3], DA Xuejuan[4], YI Fan[5], XIA Guoqing[1], LI Gaojie[1], CHEN Lan[4], JIAO Haijing[6] and WU Chihua[6]

[1] *Institute of Sedimentary Geology, Chengdu University of Technology, Chengdu 610059, China*
[2] *Institute of Geological Mechanics, Chinese Academy of Geological Sciences, Beijing 100081, China*
[3] *Key Laboratory of Paleomagnetism and Tectonic Reconstruction of Ministry of Natural Resources, Beijing 100037, China*
[4] *Department of Earth Sciences, Chongqing University of Science and Technology, Chongqing 401331,China*
[5] *College of Earth Sciences, Chengdu University of Technology, Chengdu 610059, China*
[6] *School of Marine Sciences, Sun Yat-sen University, Guangzhou 510006, China*

Citation: Yi et al., 2019. The Greenhouse Climate Records from Organic Carbon Isotope Excursions During the Toarcian (Early Jurassic) Sediments in the Shuanghu Area, Qianghai-Tibetan Plateau. *Acta Geologica Sinica* (English Edition), 93(3): 776–777. doi:10.1111/1755-6724.13790

Objective

The organic-matter-rich oil shales outcropped at the Biluo Co area of the Qiangtang Basin in Tibet are of the Toarcian (Early Jurassic) based on the ammonite fauna (Yi et al., 2003). We first proposed its sedimentary age to be the Early Toarcian and correlated with the Posidonia shales and the early Toarcian Oceanic Anoxic Event (T-OAE) (Chen et al., 2005). The carbon isotopes excursions and Buchi bivalves suggest that these oil shales at the Biluo Co section are represent of T-OAE in the Asian Tethyan regions. However, this study indicates that the anoxic environments have only involves organic matter preservation, and organic matter enrichments may be related to the appearance of greenhouse climate.

Methods

The sampling profile is located in the south-east Biluo Co and about 45 km far away from the Shuanghu County. We focused on the lowest part of this 32-m-thick section and aimed at the paleo-climates and environments of the oil shales according to the high-resolution carbon isotope curves of 53 samples. The TOC contents vary from 0.22% to 3.96%, and the samples are characterized by calcareous nannofossils and calcite crystals, which is useful to the simultaneous study of organic carbon and inorganic carbon isotope changes and their relationship (Appendix 1).

Results

The inorganic carbon isotopes ($\delta^{13}C_{Cal}$) fluctuate from −3.7‰ to 0.8‰ (relative to the PDB standard) with the maximum excursion of 4.5‰ (PDB). In contrast, the organic carbon isotopes vary from −27.7‰ to −24.9‰ (PDB) with the maximum excursion values of 2.8‰ (PDB) (Fig. 1). To show the positive and negative shift of carbon isotopes, the original data is smoothed by Moving Median. Rau et al. (1994) established the fractional equation to show the relationships between the carbon isotopes of organic matters and dissoluble CO_2 concentrations of waters, which is widely used to reconstruct the atmospheric CO_2 concentrations in Quaternary and polar ice cores. The CO_2 reconstructions were made by using the expression provided by Rau et al. (1994).

$$[CO_2\,(a)]= (\delta^{13}C_{Org}+12.6)/(-0.8) \qquad (1)$$

Where CO_2 (a) represents the CO_2 reconstructions of seawater with μmole/kg, and $\delta^{13}C_{Org}$ is relative to the PDB standard (‰). The CO_2 (a) was referenced as K_0 into P_{CO2} of sea surface atmosphere pressures with μatm close to ppmv. The solubility coefficients K_0 values are according to the temperatures and salinities of seawater. In general, the average value of salinities is 35‰, and the temperatures were estimated by applying the empirical equation:

$$T_{GAT}\ (°C)=15\ (°C)+10\times P_{CO2}/280 \qquad (2)$$

Where P_{CO2} ranging from 280 to 2800 μatm is determined by the CO_2 concentrations of sea surface and the mean temperatures of surface based on the least squares method:

$$P_{CO2}=19.542\times [CO_2(a)]^{-1.1353} \qquad (3)$$

$$T_{GAT}=4.9307\times \ln[CO_2(a)] +3.4381 \qquad (4)$$

The $\delta^{13}C_{Org}$ curves show negative excursions (Fig. 1) in the lower part (0–32 m) of oil shales at the Biluo Co section. Furthermore, the curves of P_{CO2} are characterized by continue increase according to the fractionation equation by Rau et al. (1989).

The P_{CO2} concentrations are between 440 and 500 μatm, with a mean value of 470 μatm. Additionally, the highest temperature (T_{GAT}) of Biluo Co oil shale deposition is up to 17.5°C, which indicates that the oil shales of studied area were deposited under greenhouse condition, and the higher temperature and biological bloom may be the main controlling factors for the organic-carbon-rich deposits. The $\delta^{13}C_{Cal}$ and $\delta^{13}C_{Org}$ values have the characteristics of

* Corresponding author. E-mail: yhs@cdut.edu.cn

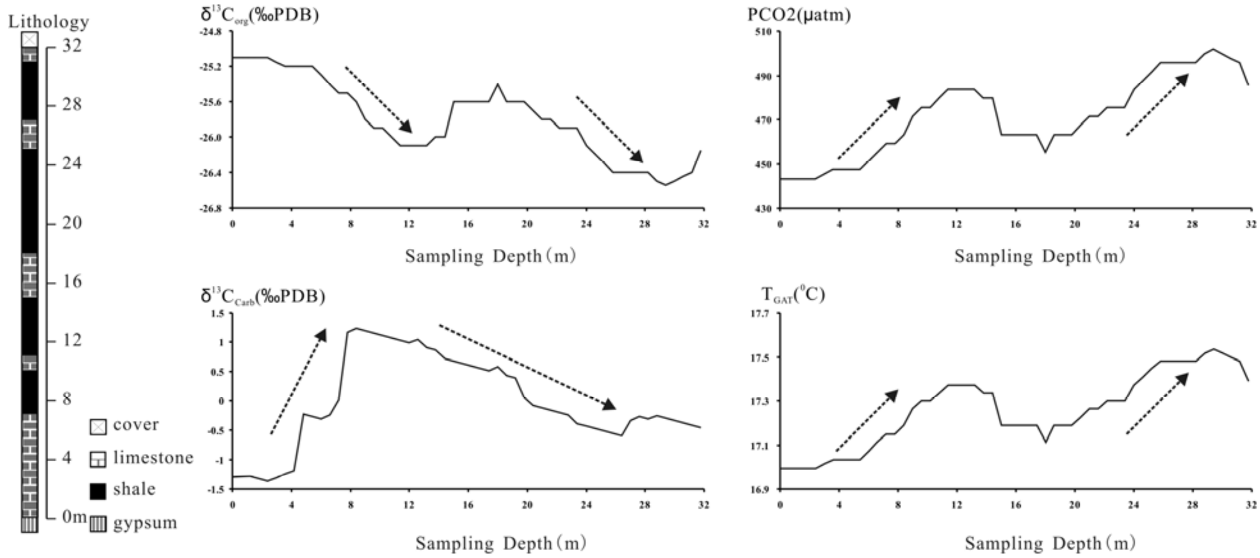

Fig. 1. The carbon isotopes and paleoclimate parameter curves of Biluocuo oil shale section in the Shuanghu area.

synchronous change showing that the $\delta^{13}C_{Cal}$ values have a negative excursion with the increase of P_{CO2}. The $\delta^{13}C$ of the carbonates and calcareous mudstones and/or shales in epicontinental sea regions have a source from the skeletons of the benthic fauna, which is an example of the Toarcian oil shale in Germany and the Qiangtang Basin, Tibet (China) with more Posidonia bivlves and less coccoliths. In general, the phytoplankton of sea surface preferentially absorbs light ^{12}C, resulting in surface seawater enrichment of ^{13}C. However, in the carbonate platform and epicontinental sea regions, benthic organisms predominate and organic matters oxygenation makes the ^{12}C rich, which may be one of the causes of the negative $\delta^{13}C_{Cal}$ excursions.

Conclusion

It is shown that the Toarcian oil shales with rich organic matters in the Qiangtang Basin, Tibet (China) were deposited under the greenhouse condition with rapidly increasing P_{CO2}. Therefore, temperatures increase and biological bloom mainly contribute to the organic matters deposition.

Acknowledgements

This work was supported by the National Natural Science Foundation of China (grants No. 41572089, 41572095 and 41602122).

References

Chen Lan, Yi Haisheng, Hu Ruizhong, Zhong Hong and Zou Yanrong, 2005. Organic Geochemistry of the Early Jurassic Oil Shale from the Shuanghu Area in Northern Tibet and the Early Toarcian Oceanic Anoxic Event. *Acta Geologica Sinica*, 79(3): 392–397 (in Chinese with English abstract).

Rau, G.H., 1994. Variations in sedimentary organic $\delta^{13}C$ as a proxy for past changes in ocean and Atmospheric CO_2 concentrations. *Nato Asi*, 17: 307–321.

Yi Haisheng, Lin Jinhui, Zhao Bing, Li Yong, Shi He, Zhu Lidong, 2003. New biostratigraphic data of the Qiangtang area in the northern Tibetan Plateau. *Geological Review,* 49(1): 59-65 (in Chinese with English abstract).

Appendix 1 Carbon isotope values of carbonate and organic matter from the Biluo Co section

Sampling Depth(m)	Sample label	$\delta^{13}C_{Carb}$(‰, PDB)	$\delta^{13}C_{org}$(‰, PDB)	Sampling Depth(m)	Sample label	$\delta^{13}C_{Carb}$(‰, PDB)	$\delta^{13}C_{org}$(‰, PDB)
0.0	BLC-001	−1.29	−25.1	16.8	BLC-053	0.56	−25.6
1.2	BLC-005	−1.28	−25.1	17.4	BLC-055	0.52	−25.6
1.8	BLC-007	−1.32	−25.1	18.0	BLC-057	0.58	−25.4
2.4	BLC-009	−1.37	−25.1	18.6	BLC-059	0.44	−25.6
3.0	BLC-011	−1.31	−25.2	19.2	BLC-061	0.40	−25.6
3.6	BLC-013	−1.25	−25.2	19.8	BLC-062	0.05	−25.6
4.2	BLC-015	−1.19	−25.2	20.4	BLC-065	−0.09	−25.7
4.8	BLC-017	−0.23	−25.2	21.0	BLC-067	−0.13	−25.8
5.4	BLC-019	−0.27	−25.2	21.6	BLC-069	−0.17	−25.8
6.0	BLC-021	−0.31	−25.3	22.2	BLC-071	−0.21	−25.9
6.6	BLC-022	−0.25	−25.4	22.8	BLC-072	−0.25	−25.9
7.2	BLC-023	0.01	−25.5	23.4	BLC-073	−0.39	−25.9
7.8	BLC-025	1.17	−25.5	24.0	BLC-075	−0.43	−26.1
8.4	BLC-027	1.23	−25.6	24.6	BLC-077	−0.47	−26.2
9.0	BLC-029	1.19	−25.8	25.2	BLC-079	−0.51	−26.3
9.6	BLC-031	1.15	−25.9	25.8	BLC-081	−0.55	−26.4
10.2	BLC-033	1.11	−25.9	26.4	BLC-083	−0.59	−26.4
10.8	BLC-035	1.07	−26.0	27.0	BLC-085	−0.33	−26.4
11.4	BLC-036	1.02	−26.1	27.6	BLC-087	−0.27	−26.4
12.0	BLC-038	0.98	−26.1	28.2	BLC-089	−0.31	−26.4
12.6	BLC-040	1.04	−26.1	28.8	BLC-091	−0.26	−26.5
13.2	BLC-042	0.90	−26.1	29.4	BLC-095	−0.30	−26.6
13.8	BLC-044	0.86	−26.0	30.0	BLC-097	−0.34	−26.5
14.4	BLC-046	0.72	−26.0	30.6	BLC-099	−0.38	−26.5
15.0	BLC-048	0.68	−25.6	31.2	BLC-101	−0.42	−26.4
15.6	BLC-050	0.64	−25.6	31.8	BLC-102	−0.46	−26.2
16.2	BLC-052	0.60	−25.6				